Hsa_circ_0008500 acts as a hsa-miR-1273h-5p sponge to protect ADSCs from apoptosis in repairing diabetic wounds by upregulation of ELK1

fandong meng
Cheeloo College of Medicine,Shandong University
fengjie shen
The Affiliated Hospital of Xuzhou Medical University
xuan chu
The Affiliated Hospital of Xuzhou Medical University
hongwei ling
The Affiliated Hospital of Xuzhou Medical University
yun qiao
Qilu Hospital of Shandong University
deshan liu (liudeshan@sdu.edu.cn)
Qilu Hospital of Shandong University

Research Article

Keywords: hsa_circ_0008500, hsa-miR-1273h-5p, ELK1, ADSCs

Posted Date: March 17th, 2022

DOI: https://doi.org/10.21203/rs.3.rs-1427635/v1

Abstract

Preliminary researches have confirmed that the number of apoptosis of adipose tissue-derived stem cells (ADSCs) in patients with diabetes is significantly increased, leading to difficulty healing a wound. More and more researches revealed that the circular RNAs (circRNAs) take part in controlling apoptosis. Whereas, if and how circRNAs are critical for regulating ADSCs apoptosis remain unknown. In this study, we utilized *in vitro* model in which ADSCs were cultivated with normal glucose (NG) (5.5 mM) or high glucose (HG) (25 mM) medium, respectively, and found that contrast to ADSCs in NG medium, more apoptotic ADSCs were observed in HG medium. In further study, we found that hsa_circ_0008500 attenuated HG-mediated ADSCs apoptosis. In addition, Hsa_circ_0008500 could directly interacted with hsa-miR-1273h-5p, acting as a miRNA sponge, which subsequently suppressed ELK1 expression, the downstream target of hsa-miR-1273h-5p. Thus, these results indicated that targeting the hsa_circ_0008500/ hsa-miR-1273h-5p/ELK1 signaling caspase in ADSCs may be an underlying treatment target for repairing diabetic wounds.

1. Introduction

Diabetes is a growing public health concern with an elevating morbidity speculated at 110 million individuals in PRC, leading to longterm high blood glucose and a variety of degeneration complications (1). Impaired wound healing (2) especial chronic foot ulcers (3), was often observed in about 5–8% of T2DM sufferers. Patients with diabetic foot ulcers(DFUs) usually exhibit unsatisfactory prognoses and a great risk of major amputation as well as premature death(4). The standard treatment for diabetic ulcers has been established. Despite the fact that novel treatment approaches have been put forward, the outcomes are still not ideal. Therefore, more valid therapeutic regimens need to be established.

Cell-based regimens are prospective for DFUs treatment, preventing amputation in sufferers (5; 6). ADSCs are stemmed from lipid tissue matrix, which can possibly affect wound therapies in non-diabetes situations, whereas they have no effects on diabetes sufferers(7). Elevated programmed cell death in stem cells is thought to damage wound repair in a diabetes rat model(8), but the precise mechanism of apoptosis remains to be investigated. Revealing the causal link beneath the programmed cell death of ADSCs might give rise to approaches for reducing apoptosis, which would help to enhance diabetic wound repair.

Recently, circRNAs have been revealed to be vital molecules in genetic expression modulation on the post-transcription level(9). CircRNAs are derived from a non-canonical form of variable splicing, usually where the splice donor spot of one exon is ligated to the splice acceptor spot of an up stream exon(10; 11). Diverse from linearity RNA, circRNA produces a continuous steady loop framework in the absence of 5’cap or 3’tail, which promotes its resistant feature to exonuclease digestion(12). The biofunction of circRNAs is versatile, changing greatly from the location, binding spots and behavior patterns of circRNAs(13). Andreeva(14) reported that circRNAs existed extensively in cellular tissue of plants and animals and had various special features biologically. Many circRNAs (namely, circRNA_0054633,

circHIPK3, circANKRD36, and circRNA11783-2) have been discovered to be related to the onset and development of diabetic diseases(15).

Recently, researches have evidenced that certain types of circRNA expressing decreases in DFUs (16; 17). Nevertheless, the effects of hsa_circ_0008500 on regulating ADSCs are still elusive. Herein, our team highlighted the effects of hsa_circ_0008500 on ADSCs and found that hsa_circ_0008500 functioning as a sponge of miR-1273h-5p to upregulate ELK1 protects ADSCs against apoptosis in repairing diabetic wound.

2. Materials And Methods

2.1. Human ADSCs isolation and culture

ADSCs were donated by Qiang Li. Lipid tissular specimens were acquired from 3 liposuction samples of sufferers with informed consent at the Affiliated Hospital of Xuzhou Medical University. To acquire stem cells, our team adopted the approaches from Zuk PA(18). Separated ADSCs were kept within L-Dulbecco's modified Eagle's medium (DMEM) (Invitrogen, America) involving 10% fetal bovine serum (FBS) (Invitrogen) under 37°C humidified incubating device at 5% CO2.

2.2. Cell treatment

ADSCs were cultivated with NG (5.5 mM) or HG (25 mM; Invitrogen, America) intermediary for 24 h. Plasmid pCMV hsa_circ_0008500 containing human hsa_circ_0008500 gene sequence was purchased from Openbiosystems, and the lentiviral vector was purchased from Shanghai Jikai Gene Company.

2.3. Flow cytometer assay

Annexin V-FITC/PI compound staining was finished to identify programmed cell death. Posterior to 48 h, Annexin V-FITC/Propidium Iodide tool (BD Biosciences) was employed to dye the cells as per the supplier's specification. After that, the specimens were studied via a flow cytometry analyzer (Attune NxT, Thermo Fisher, USA). The entire experiments were performed in triplicate.

2.4. TUNEL

To evaluate programmed cell death within cells in the face of blood sugar, TUNEL dyeing was completed as per the supplier's specification (Beyotime Institute of Biological Technology, PRC). The cells were cleaned for two times in cold PBS, subjected to fixation in 4% PFA for 0.5 h, cleaned once in PBS and afterwards subjected to permeabilization in 0.1% Triton X-100 in 0.1% Na-citrate for 120 s on ice. After that, 50 mL of TUNEL dyeing liquor was supplemented into the wells, and the cells were cultivated under 37°C for 60 min in a moist air without light. Subsequently, the programmed cell death was identified via a fluorescent microscopic device, and the apoptosis rate was studied.

2.5. RNA extraction and qPCR

Total RNA was extracted by Trizol (15596-018, Invitrogen, New York, California, USA) according to the manufacturer's instructions. 500ng of total RNA was converted into cDNA via reverse transcription through the PrimeScript RT Master Mix (TaKaRa, PRC). The comparative RNA expressing was tested via the SYBR Premix Ex Taq II Kit (TaKaRa, PRC) on the StepOnePlus system (Applied Biosystems, America). The data were computed via the 2 − ΔΔCt approach(19).

2.6. WB assay

Proteins were abstracted via RIPA cellular lysis buffering solution (Beyotime, PRC). 10 μg of proteins were subjected to SDS-PAGE and moved onto PVDF films (Hybond; America). The films were subjected to blockade for 60 min via 5% milk and afterwards probed with the first antisubstances and the proper second antisubstances (CST, America). Eventually, WB was identified via a chemiluminescent reagent tool (Merck KGaA, Germany).

2.7. Luciferase reporter gene assay

Hsa_circ_0008500 WT and MUT sequences were cloned down stream of the FFL gene pGL3 vector (Promega, America). Hsa-miR-1273h-5p expressing plasmids(pmirGLO) were cotransfected with FFL-reporter plasmids in a transient way (Promega) via liposome transfection 2000 as per the supplier's specification. After that, pGL3- Hsa_circ_0008500 vectors were cotransfected with hsa-miR-1273h-5p mimetic substances and NC into ADSCs. Posterior to 24 hours, Dual-luciferase Reporter Genetic Analysis Tool (Promega) was employed to identify the fluorescein enzyme activity as per the supplier's specification. The comparative FFL activities were standardized to the Renilla fluorescein enzyme activities.

2.8. RNA pull-down assay

ADSCs, stably transfected with circ0008500 or NC, were lysed and cultivated via special probes. The biotin-coupled RNA complex in cellular lysates was pulled down by magnet beads coated with streptavidin (TFS). The miR-1273h-5p level in the bound fraction was assessed via qRT-PCR.

2.9. RNA-binding protein immunoprecipitation (RIP) assay

RIP assays were completed via the aMagna RIP RNA-binding protein immune precipitation tool (Merck Millipore). ADSCs were collected 24h posterior to the transfection of hsa-miR-1273h-5p mimetic substances or miR-NC and lysed in RNA lysis buffering solution. The cellular lysates were cultivated with antisubstance-conjugated magnet beads (AGO2 or IgG antisubstance, (CST, America) in 4°Cfor 4h. The beads were subjected to treatment as per the supplier's specification. The coprecipitated RNA was subjected to purification and identified via qRT-PCR.

2.10. Fluorescence in situ hybridisation analysis

The subcell localisation of hsa_circ_0008500 and hsa-miR-1273h-5p was determined via FISH method as per the specification from the RiboTM lncRNA FISH Probe Mix (Red) (RiboBio, PRC). Specifically, the cells were seeded into a 24-well dish at 6 × 104 cells per well till 85% confluence, acquired and subjected to

fixation in 1 mL of 4% PFA under RT. Posterior to the exposure to 50 μL of pre-hybridisation liquor for one night. cells were cleaned for two times in PBST and dyed in DAPI (1: 800) for 300 s the next day. Posterior to PBST cleaning, the cells were mounted with antifade reagent, studied and imaged via a fluorescent microscopic device (Olympus, Japan). Eventually, 5 diverse fields of view were stochastically selected for study and imaging.

2.11. Statistics

Statistic assay was completed via GraphPad Prism 6 and SPSS v. 19. Remarkable diversity on statistics was computed via t-test for two-group comparison with the controls or via ANOVA for multi-comparison amongst groups. $P < 0.05$ had significance on statistics.

3. Result

3.1. The expression of hsa_circ_0008500 was downregulated under high glucose

CircRNAs have been reported to regulate apoptosis signaling in many cells during diabetes(16; 20–23). As shown in Fig. 1, compared with normal glucose control, the high glucose group was apparently decreased in serum content of hsa_circ_0008500. And the expressing level of hsa_circ_0008500 was concentration-dependent and time-dependent (Fig. 1A, B). Then we decided to focus on hsa_circ_0008500(Fig. 1C). Hsa_circ_0008500 was merely magnified by different primers in cDNA, and no magnification products were identified in gDNA (Fig. 1D). Moreover, hsa_circ_0008500 was resistant to RNase R, whereas hsa_circ_0008500 mRNA was remarkably decreased posterior to the treatment with RNase R (Fig. 1E). Taken together, those discoveries revealed that the expressing of hsa_circ_0008500 decreases in ADSCs under high glucose.

3.2. The apoptosis of ADSCs were increased in HG condition

To explore the mechanism of ADSCs programmed cell death in diabetic wounds, ADSCs were exposed to high glucose (25mM, 40mM, 80mM) for (12h, 24h, 48h). Flow cytometry analysis of cell apoptosis showed that the apoptosis of diabetic ADSCs increased significantly (Fig. 2A, B). Subsequently, our team utilized a TUNEL tool to identify programmed cell death and acquired alike outcomes (Fig. 2C, D). WB unraveled that the expressing of the proapoptotic molecule BAX was elevated and the expression of the antiapoptotic protein BCL-2 decreased under high glucose (Fig. 2E, F). Collectively, those outcomes unveiled that the glucotoxicity milieu accelerated the apoptosis of ADSCs.

3.3. Overexpression of hsa_circ_0008500 suppressed HG-triggered apoptosis of ADSCs.

Our team identified increased apoptotic ADSCs in high-glucose conditions (Fig. 2A, B). After co-culturing hsa_circ_0008500 with ADSCs, our team leveraged flow cell technique to identify ADSC programmed cell death, revealing a significantly reduced apoptosis rate in the identical HG milieu posterior to co-culture (Fig. 2A, B). Subsequently, our team employed a TUNEL tool to identify programmed cell death and acquired alike outcomes (Fig. 2C, D). WB unraveled that the expressing of proapoptotic molecule BAX was reduced with the elevation of hsa_circ_0008500, and the expressing of antiapoptotic protein BCL-2 was elevated with the elevation of hsa_circ_0008500 (Fig. 2E, F), confirming that hsa_circ_0008500 could reduce apoptosis of ADSCs within a HG milieu.

3.4. Hsa_circ_0008500 decoys hsa-miR-1273h-5p as a sponge RNA.

we used RNA-FISH to detect the cellular localisation of hsa_circ_0008500. hsa_circ_0008500 was also primarily located in the cytoplasm (Fig. 3A). Subsequently, to identify the causal link where hsa_circ_0008500 modulates ADSCs programmed cell death, our team finished qPCR to identify the localization of hsa_circ_0008500 (Fig. 3B). Hsa_circ_0008500 was primarily located in the cytoplasm, which revealed that it might compete with endogenetic RNA and could be a molecule sponge for miRNA. A searching of the data base identified the 3 miRNAs with the greatest binding scoring. we overexpressed hsa_circ_0008500 in the ADSCs and measured these miRNAs. Only hsa-miR-1273h-5p was significantly downregulated by hsa_circ_0008500 in ADSCs (Fig. 3C). Moreover, our team forecasted the potential binding spots of hsa_circ_0008500 in hsa-miR-1273h-5p and established WT and MUT fluorescein enzyme reporter genes. The hsa-miR-1273h-5p mimic reduced hsa_circ_0008500 WT reporter levels, but it did not affect hsa_circ_0008500 MUT reporter levels (Fig. 3D). Hsa_circ_0008500 RNA pull-down analysis revealed that hsa_circ_0008500 probes could enrich hsa-miR-1273h-5p (Fig. 3E).

MiRNA inhibits the expression of its target via Argonaute RISC catalytic component 2 (AGO2). Thus, our team utilized an RNA pull-down method to identify if hsa_circ_0008500 binds AGO2. As demonstrated by WB, compared with antisense control, hsa_circ_0008500 could bind to AGO2 (Fig. 3F). RIP analysis was also completed to assess the mutual effect between hsa_circ_0008500 and hsa-miR-1273h-5p. To evaluate the binding mechanism of hsa_circ_0008500 and hsa-miR-1273h-5p, anti-AGO2 RIP was completed in ADSCs overexpressing hsa-miR-1273h-5p. Cells transfected with hsa-miR-1273h-5p were enriched with endogenetic hsa_circ_0008500 by AGO2 in a specific way (Fig. 3G), revealing that hsa-miR-1273h-5p could be a hsa_circ_0008500-carrying miRNA. These findings support the notion that hsa_circ_0008500 is like a sponge for hsa-miR-1273h-5p. AGO2-RIP assay showed that hsa_circ_0008500 binds to the AGO2 protein (Fig. 3H).

3.5. MiR-1273h-5p advanced ADSCs apoptosis through targeting ELK1.

Because hsa_circ_0008500 and hsa-miR-1273h-5p have a competitive endogenous relationship, hsa_circ_0008500 promotes apoptosis by targeting hsa-miR-1273h-5p. To study the role of hsa-miR-1273h-5p in apoptosis in depth, hsa-miR-1273h-5p -mimetic substances were transferred into the cells.

Flow cytometry (Fig. 4C, D) and TUNEL (Fig. 4E, F) revealed increased apoptosis in the hsa-miR-1273h-5p-mimics group under high-glucose stress. Western blot results revealed that BAX expression increased with hsa-miR-1273h-5p -mimics transfection under high-glucose stress, while BCL-2 and ELK1expression decreased (Fig. 4G, H). Those discoveries suggest that hsa-miR-1273h-5p alleviates ADSC apoptosis. To reveal the cytoprotective mechanism of hsa-miR-1273h-5p, we predicted the down stream targets of hsa-miR-1273h-5p through miRDB miRNA target forecast. Our team chose ELK1, as it is a known regulator of apoptosis. To determine if hsa-miR-1273h-5p targets ELK1, our team cloned the 3'UTR sequence of ELK1 into the psiCHECK™-2 vector and established a MUT 3'-UTR reporter that had no hsa-miR-1273h-5p binding site (Fig. 4A). Introduction of hsa-miR-1273h-5p diminished the fluorescein enzyme activity of ELK1 3'-UTR reporter, while MUT ELK1 3'-UTR reporter gene activity remained unchanged (Fig. 4B). qPCR and WB assays identified that hsa-miR-1273h-5p downregulated ELK1 mRNA and protein (Fig. 4H, I). Collectively, those discoveries unveiled that hsa-miR-1273h-5p straightly targeted the ELK1 3'-UTR, downregulating ELK1 expression and inhibiting ADSC apoptosis in high-glucose stress.

3.6. Hsa_circ_0008500 regulates ADSCs apoptosis via hsa-miR-1273h-5p.

Our team investigated in depth if hsa-miR-1273h-5p participated in the modulation of programmed cell death by hsa_circ_0008500 under HG conditions. Our team performed the co-transfection of ADSCs with hsa-miR-1273h-5p mimics and a hsa_circ_0008500 overexpression vector. Flow cytometry revealed that hsa-miR-1273h-5p mimics significantly increased apoptosis caused by hsa_circ_0008500 overexpression (Fig. 5A, B). TUNEL (Fig. 5C, D) and WB analyses (Fig. 5E, F) revealed consistent results. Collectively, those discoveries unveiled that hsa_circ_0008500 regulates high-glucose-induced ADSC apoptosis through hsa-miR-1273h-5p /ELK1.

4. Discussion

Since ADSCs is imperative for wound healing, its pivotal to unravel the potential molecule-level causal links of increased apoptosis of ADSCs in patients with diabetes. To date, Circular RNAs have been associated with multiple mankind illnesses, such as diabetic diseases, heart and blood vessel illnesses, persistent inflammation illnesses and neurological disorders(24–27). There are few previous studies on hsa_circ_0008500. Only one study indicates that hsa_circ_0008500 is like a miR-1301-3p sponge to facilitate osteoblastic cell mineralisation via the upregulation of PADI4(28). Herein, hsa_circ_0008500 was focused on. Our results of qRT-PCR revealed that hsa_circ_0008500 was regulated downward in ADSCs at HG in vitro. In addition, our team overexpressed hsa_circ_0008500 in diabetic ADSCs, and it was discovered that the programmed cell death of ADSCs was remarkably decreased. The discoveries herein unveiled that hsa_circ_0008500 is able to suppress the programmed cell death of ADSCs and facilitate the healing of diabetic wounds.

Circular RNAs have diverse roles owing to diverse distributional status. To investigate the effects of hsa_circ_0008500 on the modulation of cell apoptosis in depth, our team conducted localization

experiments. Hsa_circ_0008500 was mainly distributed in the cytoplasm, and cytoplasmic CircRNA primarily operates via ceRNA. Many Circular RNAs exert important biological functions by acting as protein suppressors ('sponges') or microRNA, via modulating protein functions or via their own translation (29). After that, by virtue of biological information forecast, our team discovered that miR-1273h-5p has a hsa_circ_0008500 binding spot. miRNAs interact with the AGO protein family to inhibit translation or decompose mRNA. After that, our team integrated the RIP and RNA pull-down assays to demonstrate that hsa_circ_0008500 is capable of binding to the AGO2 protein. The luciferase reporter assay confirmed as well that hsa_circ_0008500 was able to inhibit miR-1273h-5p expression. We performed qRT-PCR in the miR-1273h-5p-mimic group, demonstrating that hsa_circ_0008500 was decreased, which confirmed that hsa_circ_0008500 decoyed miR-1273h-5p as a sponge RNA.

CircRNAs can function as ceRNA of miRNAs by regulating apoptosis in mankind illnesses(30). For example, circERCC2 could ameliorate intervertebral disc degeneration (IVDD) via miR-182-5p/SIRT1 axis through stimulating mitochondrial autophagy and suppressing programmed cell death, and reveals that circERCC2 is an underlying valid treatment target of IVDD(31). There has been evidence that mmu_circ_0000250 inhibited programmed cell death by autophagy activation, and mmu_circ_0000250 reinforced the treatment potency of ADSCs-exosomes to facilitate wound repair in diabetic diseases via absorpting miR-128-3p and upregulating SIRT1(16). The present research highlighted the effects of hsa_circ_0008500 on regulating ADSCs apoptosis under high glucose, and demonstrated that high expressing of hsa_circ_0008500 inhibited apoptosis of ADSCs. The causal link of hsa_circ_0008500 in apoptosis of ADSCs is limited and needs more exploration.

MiRNAs participate in the modulation of post-transcription genetic expression in cytobiology. Coherent with the high expressing levels of hsa-miR-1273h-5p identified herein, the expression level of hsa-miR-1273h-5p was high under high glucose conditions relative to that under normal glucose conditions. In addition, the data herein revealed that the expressing of hsa_circ_0008500 was related to the expression of hsa-miR-1273h-5p in a negative way. At the same time, the outcomes in this research greatly reveal that hsa_circ_0008500 can be a ceRNA of miR-1273h-5p to realize the downregulation of its expression. A study reported miR-1273h-5p as a contributor to gastric cancer growth and metastasis(32). MiR-1273h-5p, which was remarkably elevated within the peripheral blood monocytes of SLE sufferers, might be a new biomarker for the diagnoses and assessment of SLE(33). Since hsa_circ_0008500 sponged miR-1273h-5p as a ceRNA, our team researched the effects of miR-1273h-5p on ADSC apoptosis and discovered that miR-1273h-5p accelerated apoptosis. In addition, biological information forecast and luciferase reporter assay unveiled that miR-1273h-5p was critical negative regulator of ELK1.

We sought to elucidate the effects of miR-1273h-5p on the modulation of ADSCs apoptosis in depth ; indeed, we found that ELK1 acted as the targeted protein of miR-1273h-5p and demonstrated that miR-1273h-5p suppressed ELK1 expression. ELK1, a TF of the ETS family, is a pivotal constituent of the mitogen modulation signal path activating the mitogen-stimulated protein kinase cascade(34). ELK1 primarily participated in the modulation of cellular proliferation, differentiation, and apoptosis(35). ELK1 is vital for miR-139-3p to suppress osteoblastic differentiation and facilitate osteoblastic programmed

cell death(35). MiR-150 can modulate the expressing of ELK1, while ELK1 knockout can terminate the antiapoptotic effect of the suppressor miR-150 in endotheliocytes(36). Another study confirmed that Zuo Gui Jiang Tang Jie Yu Formula was capable of reversing the expression of ELK-1, JNK and c-Fos signals in hippocamp nerve cells in DD milieu and eserted antiapoptotic effects(37). In conclusion, we unveiled that hsa_circ_0008500 could modulate the expressing of ELK-1 via sponging miR-1273h-5p. We verified that hsa_circ_0008500 regulates ADSC apoptosis through miR-1273h-5p / ELK1, thus elucidating the mechanism of ADSC apoptosis under high-glucose stress.

5. Conclusion

Taken together, we first demonstrated that hsa_circ_0008500 realized the upregulation of ELK1 expression via sponging miR-1273h-5p, inhibiting ADSCs apoptosis. Those discoveries might deepen our knowledge as to the modulatory circRNA network and DFUs. These new data might be helpful to develop circular RNA-based diagnosis and treatment regimens for DFUs.

Declarations

Acknowledgements

Not applicable.

Data Availability

The datasets used or analyzed during the current study are available from the corresponding author on reasonable request.

Conflicts of Interest

The authors have no conflicts of interest to declare.

Funding statement

This work was supported by grants from Graduate Research and Innovation Projects of Jiangsu Province SJCX21_1142 , from State Administration of Traditional Chinese Medicine Qilu Internal Medicine School of Diseases Inheritance Studio Project (LP0115033) to D.S.L, and from Liu Deshan Shandong Province Famous and Old Traditional Chinese Medicine Expert Inheritance Studio Construction Project 2019-19 to D.S.L.

Author's contributions:

F.D.M and F.J.S performed the experiments and contributed equally to the preparation of the manuscript. X.C. wrote the manuscript. H.W. L analyzed the data. Y.Q and D.S.L contributed to the conception and design of the study.

Ethics approval and consent to participate

This research was authorized by the ethics committee of the Affiliated Hospital of Xuzhou Medical University. It is confirmed that the study was carried out in compliance with the Declaration of Helsinki. Written informed consent was acquired from every participant.

Consent for publication

Not Applicable.

Competing interests

The authors declare that they have no financial conflict of interest

References

1. Pickering RJ, Rosado CJ, Sharma A, Buksh S, Tate M, de Haan JB: Recent novel approaches to limit oxidative stress and inflammation in diabetic complications. Clin Transl Immunology 2018;7:e1016
2. Uchiyama A, Motegi SI, Sekiguchi A, Fujiwara C, Perera B, Ogino S, Yokoyama Y, Ishikawa O: Mesenchymal stem cells-derived MFG-E8 accelerates diabetic cutaneous wound healing. J Dermatol Sci 2017;86:187–197
3. Huang Z, Lu M, Zhu G, Gao H, Xie L, Zhang X, Ye C, Wang Y, Sun C, Li X: Acceleration of diabetic-wound healing with PEGylated rhaFGF in healing-impaired streptozocin diabetic rats. Wound Repair Regen 2011;19:633–644
4. Jones NJ, Harding K: 2015 International Working Group on the Diabetic Foot Guidance on the prevention and management of foot problems in diabetes. Int Wound J 2015;12:373–374
5. Soria B, Montanya E, Martin F, Hmadcha A: A Role for the Host in the Roadmap to Diabetes Stem Cell Therapy. Diabetes 2016;65:1155–1157
6. Liang L, Li Z, Ma T, Han Z, Du W, Geng J, Jia H, Zhao M, Wang J, Zhang B, Feng J, Zhao L, Rupin A, Wang Y, Han ZC: Transplantation of Human Placenta-Derived Mesenchymal Stem Cells Alleviates Critical Limb Ischemia in Diabetic Nude Rats. Cell Transplant 2017;26:45–61
7. Ohmura Y, Tanemura M, Kawaguchi N, Machida T, Tanida T, Deguchi T, Wada H, Kobayashi S, Marubashi S, Eguchi H, Takeda Y, Matsuura N, Ito T, Nagano H, Doki Y, Mori M: Combined transplantation of pancreatic islets and adipose tissue-derived stem cells enhances the survival and insulin function of islet grafts in diabetic mice. Transplantation 2010;90:1366–1373
8. Saki N, Jalalifar MA, Soleimani M, Hajizamani S, Rahim F: Adverse effect of high glucose concentration on stem cell therapy. Int J Hematol Oncol Stem Cell Res 2013;7:34–40
9. Conn SJ, Pillman KA, Toubia J, Conn VM, Salmanidis M, Phillips CA, Roslan S, Schreiber AW, Gregory PA, Goodall GJ: The RNA binding protein quaking regulates formation of circRNAs. Cell 2015;160:1125–1134

10. Zhang M, Xu K, Fu L, Wang Q, Chang Z, Zou H, Zhang Y, Li Y: Revealing Epigenetic Factors of circRNA Expression by Machine Learning in Various Cellular Contexts. iScience 2020;23:101842
11. Zhao S: Alternative splicing, RNA-seq and drug discovery. Drug Discov Today 2019;24:1258–1267
12. Chen S, Zhao Y: Circular RNAs: Characteristics, function, and role in human cancer. Histol Histopathol 2018;33:887–893
13. Liu J, Liu T, Wang X, He A: Circles reshaping the RNA world: from waste to treasure. Mol Cancer 2017;16:58
14. Andreeva K, Cooper NG: MicroRNAs in the Neural Retina. Int J Genomics 2014;2014:165897
15. Abbaszadeh-Goudarzi K, Radbakhsh S, Pourhanifeh MH, Khanbabaei H, Davoodvandi A, Fathizadeh H, Sahebkar A, Shahrzad MK, Mirzaei H: Circular RNA and Diabetes: Epigenetic Regulator with Diagnostic Role. Curr Mol Med 2020;20:516–526
16. Shi R, Jin Y, Hu W, Lian W, Cao C, Han S, Zhao S, Yuan H, Yang X, Shi J, Zhao H: Exosomes derived from mmu_circ_0000250-modified adipose-derived mesenchymal stem cells promote wound healing in diabetic mice by inducing miR-128-3p/SIRT1-mediated autophagy. Am J Physiol Cell Physiol 2020;318:C848-C856
17. Xiang Y, Kuai L, Ru Y, Jiang J, Li X, Li F, Chen Q, Li B: Transcriptional profiling and circRNA-miRNA-mRNA network analysis identify the biomarkers in Sheng-ji Hua-yu formula treated diabetic wound healing. J Ethnopharmacol 2021;268:113643
18. Tamama K, Kawasaki H, Wells A: Epidermal growth factor (EGF) treatment on multipotential stromal cells (MSCs). Possible enhancement of therapeutic potential of MSC. J Biomed Biotechnol 2010;2010:795385
19. Schefe JH, Lehmann KE, Buschmann IR, Unger T, Funke-Kaiser H: Quantitative real-time RT-PCR data analysis: current concepts and the novel "gene expression's CT difference" formula. J Mol Med (Berl) 2006;84:901–910
20. Liu Y, Chen X, Yao J, Kang J: Circular RNA ACR relieves high glucose-aroused RSC96 cell apoptosis and autophagy via declining microRNA-145-3p. J Cell Biochem 2019;
21. Wei H, Cao C, Wei X, Meng M, Wu B, Meng L, Wei X, Gu S, Li H: Circular RNA circVEGFC accelerates high glucose-induced vascular endothelial cells apoptosis through miR-338-3p/HIF-1alpha/VEGFA axis. Aging (Albany NY) 2020;12:14365–14375
22. An L, Ji D, Hu W, Wang J, Jin X, Qu Y, Zhang N: Interference of Hsa_circ_0003928 Alleviates High Glucose-Induced Cell Apoptosis and Inflammation in HK-2 Cells via miR-151-3p/Anxa2. Diabetes Metab Syndr Obes 2020;13:3157–3168
23. Wang Y, Qi Y, Ji T, Tang B, Li X, Zheng P, Bai S: Circ_LARP4 regulates high glucose-induced cell proliferation, apoptosis, and fibrosis in mouse mesangial cells. Gene 2021;765:145114
24. Hanan M, Soreq H, Kadener S: CircRNAs in the brain. RNA Biol 2017;14:1028–1034
25. Meng J, Chen S, Han JX, Qian B, Wang XR, Zhong WL, Qin Y, Zhang H, Gao WF, Lei YY, Yang W, Yang L, Zhang C, Liu HJ, Liu YR, Zhou HG, Sun T, Yang C: Twist1 Regulates Vimentin through Cul2 Circular

RNA to Promote EMT in Hepatocellular Carcinoma. Cancer Res 2018;78:4150–4162

26. Holdt LM, Stahringer A, Sass K, Pichler G, Kulak NA, Wilfert W, Kohlmaier A, Herbst A, Northoff BH, Nicolaou A, Gabel G, Beutner F, Scholz M, Thiery J, Musunuru K, Krohn K, Mann M, Teupser D: Circular non-coding RNA ANRIL modulates ribosomal RNA maturation and atherosclerosis in humans. Nat Commun 2016;7:12429
27. Aufiero S, Reckman YJ, Pinto YM, Creemers EE: Circular RNAs open a new chapter in cardiovascular biology. Nat Rev Cardiol 2019;16:503–514
28. Zhai Q, Zhao Y, Wang L, Dai Y, Zhao P, Xiang X, Liu K, Du W, Tian W, Yang B, Li T, Wang L: CircRNA hsa_circ_0008500 Acts as a miR-1301-3p Sponge to Promote Osteoblast Mineralization by Upregulating PADI4. Front Cell Dev Biol 2020;8:602731
29. Ebbesen KK, Kjems J, Hansen TB: Circular RNAs: Identification, biogenesis and function. Biochim Biophys Acta 2016;1859:163–168
30. Tay Y, Rinn J, Pandolfi PP: The multilayered complexity of ceRNA crosstalk and competition. Nature 2014;505:344–352
31. Xie L, Huang W, Fang Z, Ding F, Zou F, Ma X, Tao J, Guo J, Xia X, Wang H, Yu Z, Lu F, Jiang J: CircERCC2 ameliorated intervertebral disc degeneration by regulating mitophagy and apoptosis through miR-182-5p/SIRT1 axis. Cell Death Dis 2019;10:751
32. Dong XZ, Zhao ZR, Hu Y, Lu YP, Liu P, Zhang L: LncRNA COL1A1-014 is involved in the progression of gastric cancer via regulating CXCL12-CXCR4 axis. Gastric Cancer 2020;23:260–272
33. Guo G, Wang H, Shi X, Ye L, Wu K, Lin K, Ye S, Li B, Zhang H, Lin Q, Ye S, Xue X, Chen C: NovelmiRNA-25 inhibits AMPD2 in peripheral blood mononuclear cells of patients with systemic lupus erythematosus and represents a promising novel biomarker. J Transl Med 2018;16:370
34. Sharrocks AD: The ETS-domain transcription factor family. Nat Rev Mol Cell Biol 2001;2:827–837
35. Wang Y, Wang K, Hu Z, Zhou H, Zhang L, Wang H, Li G, Zhang S, Cao X, Shi F: MicroRNA-139-3p regulates osteoblast differentiation and apoptosis by targeting ELK1 and interacting with long noncoding RNA ODSM. Cell Death Dis 2018;9:1107
36. Ying W, Tseng A, Chang RC, Wang H, Lin YL, Kanameni S, Brehm T, Morin A, Jones B, Splawn T, Criscitiello M, Golding MC, Bazer FW, Safe S, Zhou B: miR-150 regulates obesity-associated insulin resistance by controlling B cell functions. Sci Rep 2016;6:20176
37. Liu Z, Liu J, Ling J, Yang Q, Yang H, Meng P, Du Q, Zhao HQ, Wang YH: [Effects of ELK-1/JNK/c-Fos on apoptosis of rat hippocampal neurons cultured in vitro with Zuogui Jiangtang Jieyu Formula in simulated diabetes mellitus complicated with depression]. Zhongguo Ying Yong Sheng Li Xue Za Zhi 2019;35:50–54

Figures

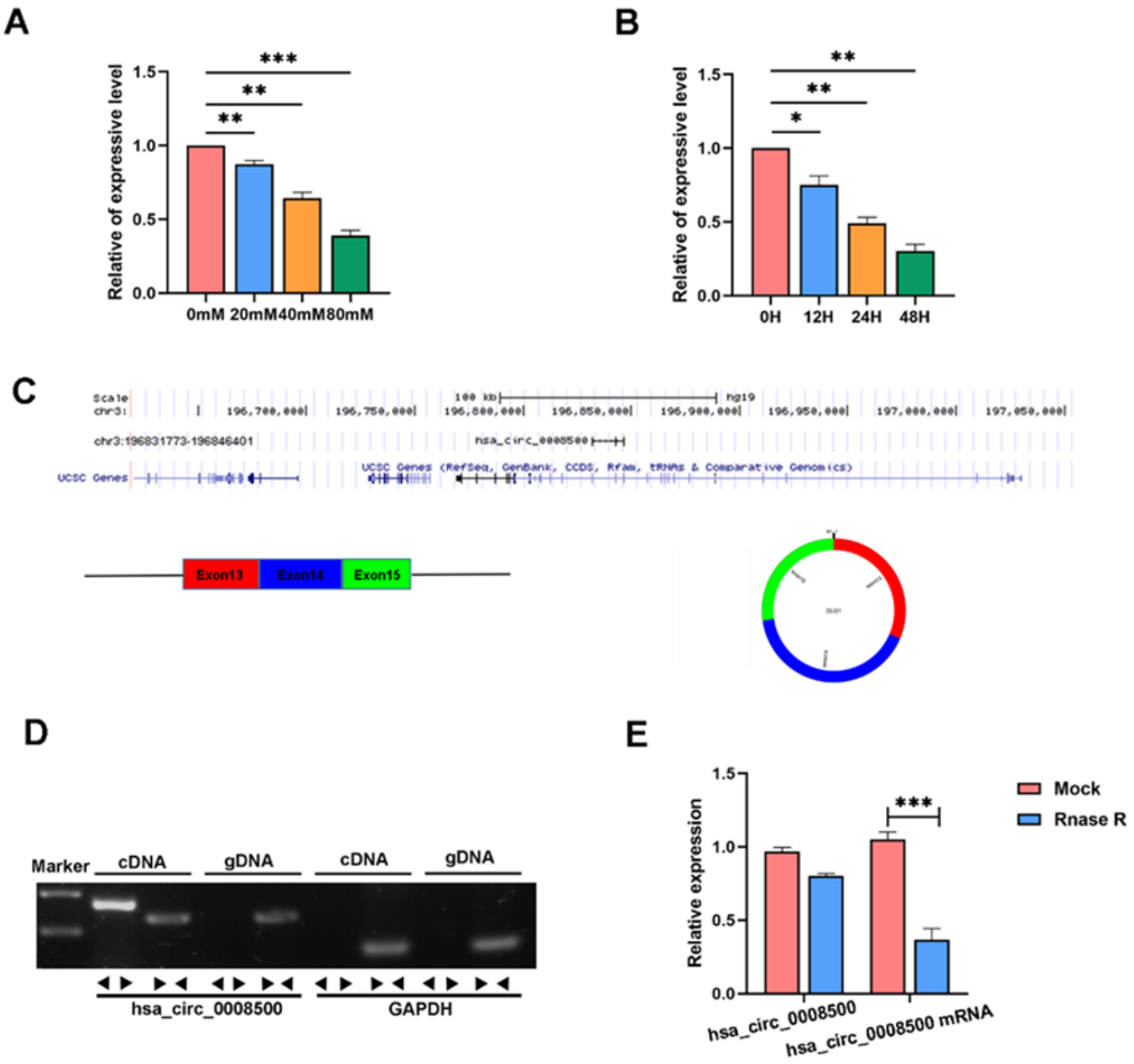

Figure 1

Hsa_circ_0008500 is downregulated in high glucose treated ADSCs. A. The comparative expressing level of hsa_circ_0008500 in ADSCs was detected under different concentrations of high glucose environment. B. The comparative expressing level of hsa_circ_0008500 at different time after high glucose treatment. C. Schematic diagram of hsa_circ_0008500 structure. D. The presence of hsa_circ_0008500 was verified in ADSCs lines via RT-PCR. E. The expressions of hsa_circ_0008500 and hsa_circ_0008500 mRNA in ADSCs treated with or without RNase R were detected via qRT-PCR. Data were presented as average ± SD, n = 3. **P< 0.01. ***P< 0.001.

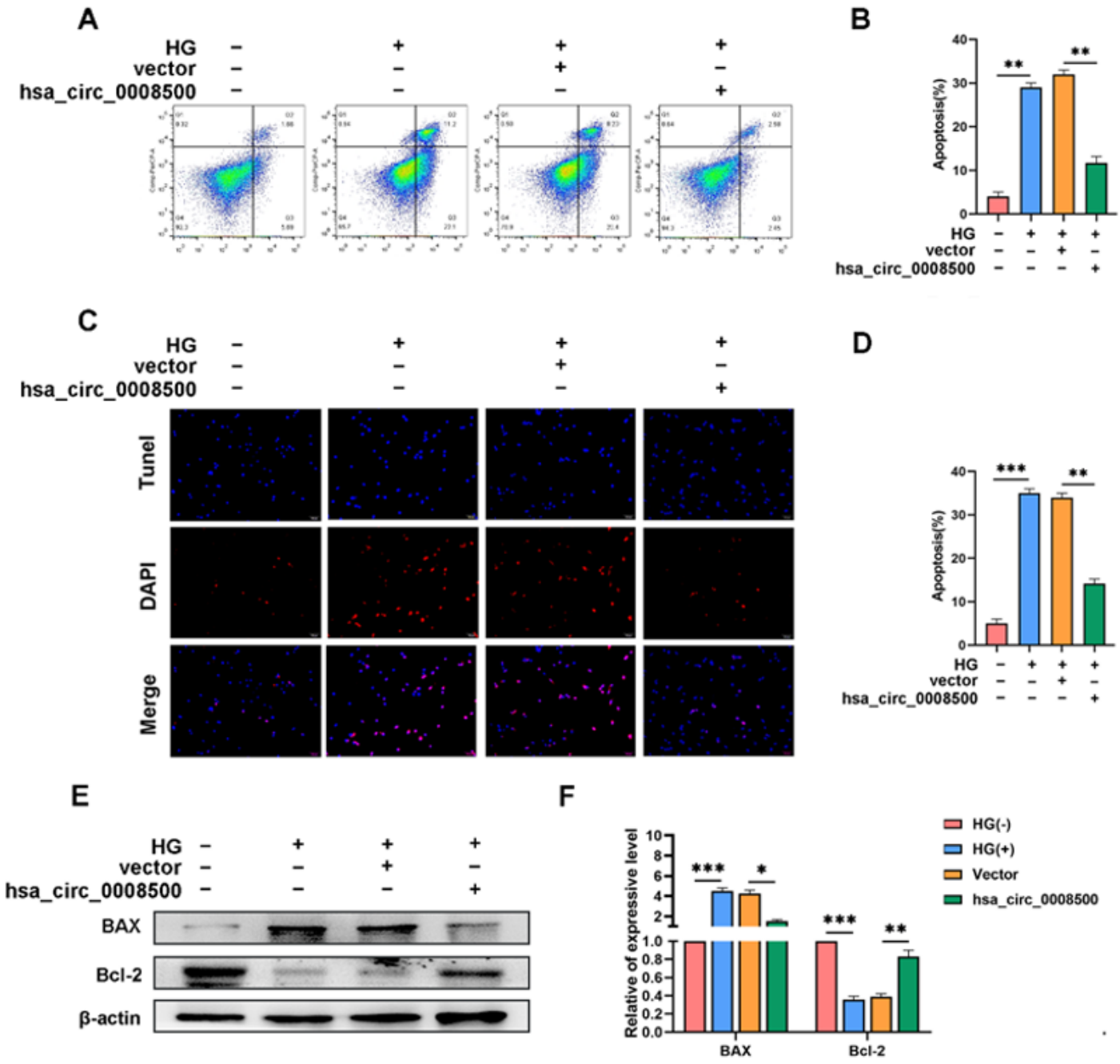

Figure 2

Hsa_circ_0008500 regulated ADSCs programmed cell death under HG. ADSCs were treated with HG or NG in hsa_circ_0008500 overexpressing ADSCs or control cells. A, B. Cells were stained with Annexin PE/7-AAD and directly studied via flow cell technique. C, D. Typical TUNEL dyeing image of ADSCs. E F. The protein content of Bcl-2 and Bax was identified via WB. Data were presented as average ± SD of 3 independently performed assays. **P< 0.01 ***P< 0.001.

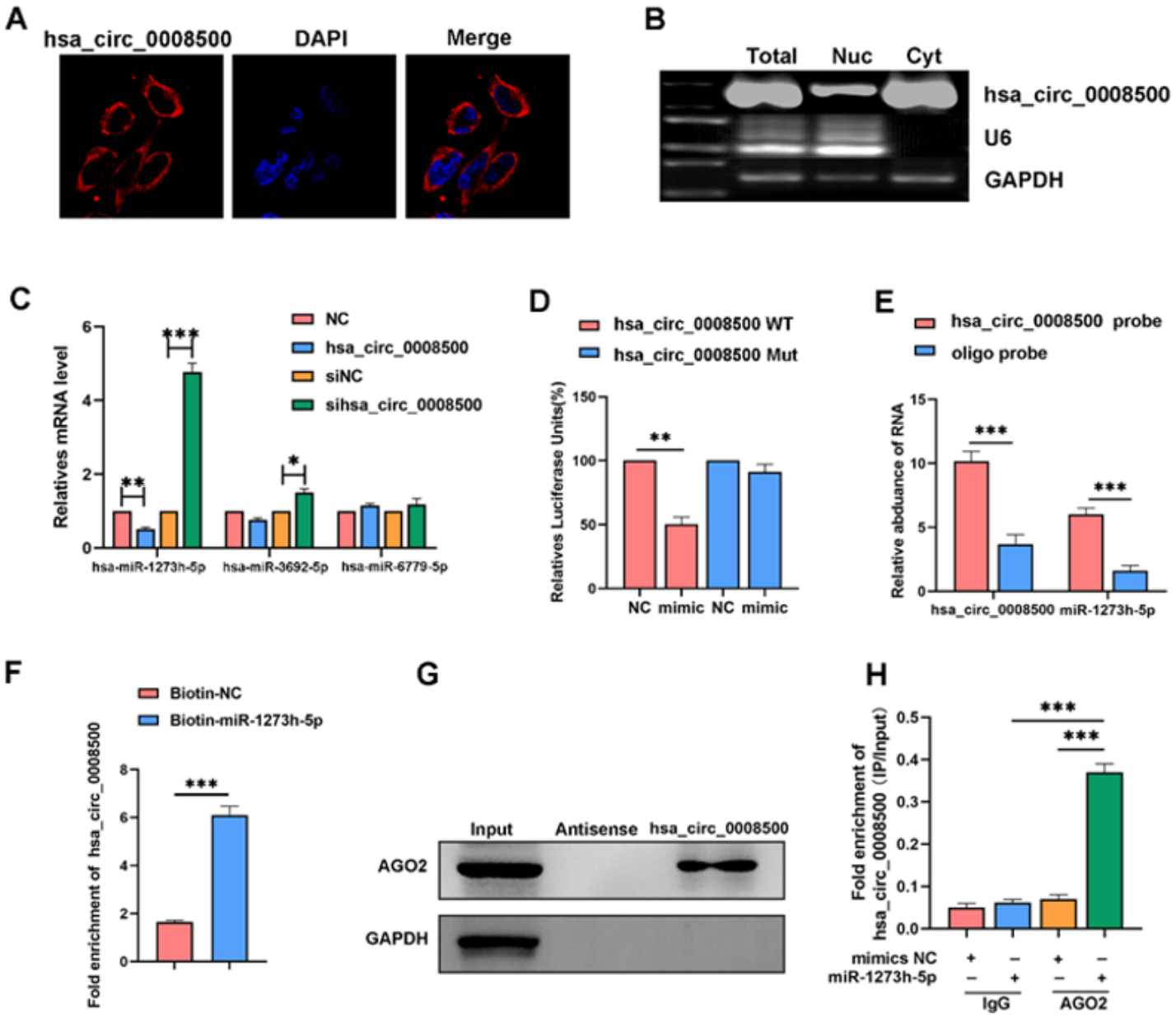

Figure 3

Hsa_circ_0008500 decoys hsa-miR-1273h-5p as a sponge RNA. A. FISH detection for hsa_circ_0008500 (red)was performed in (scale bar =20 μm). The nuclei were subjected to counterstaining via DAPI (blue). The merge images displayed that hsa_circ_0008500 was primarily colocalized in the cytoplasm. B. RT-PCR was used to identify the relative expression levels of hsa_circ_0008500, U6 and GAPDH in nuclei, cytoplasm and whole cells of ADSCs. C. In the downregulated and overexpression groups of hsa_circ_0008500, qRT-PCR was used to identify the expressing of microRNAs screened out. D. Relative fluorescein enzyme activities of WT and MUT hsa_circ_0008500. E. Hsa_circ_0008500 was enriched with hsa_circ_0008500 specific probe, and then hsa_circ_0008500 and hsa-miR-1273h-5p were identified via qRT-PCR. F. The biotinylation hsa-miR-1273h-5p was introduced into cells via transfection. Posterior to streptavidin capture, hsa_circ_0008500 levels were quantified by qRT-PCR. G. RNA pull-down test

analyzed the interaction between hsa_circ_0008500 and AGO2. H. RIP test analyzed the mutual effect between hsa_circ_0008500 and AGO2. **P< 0.01, ***P< 0.001.

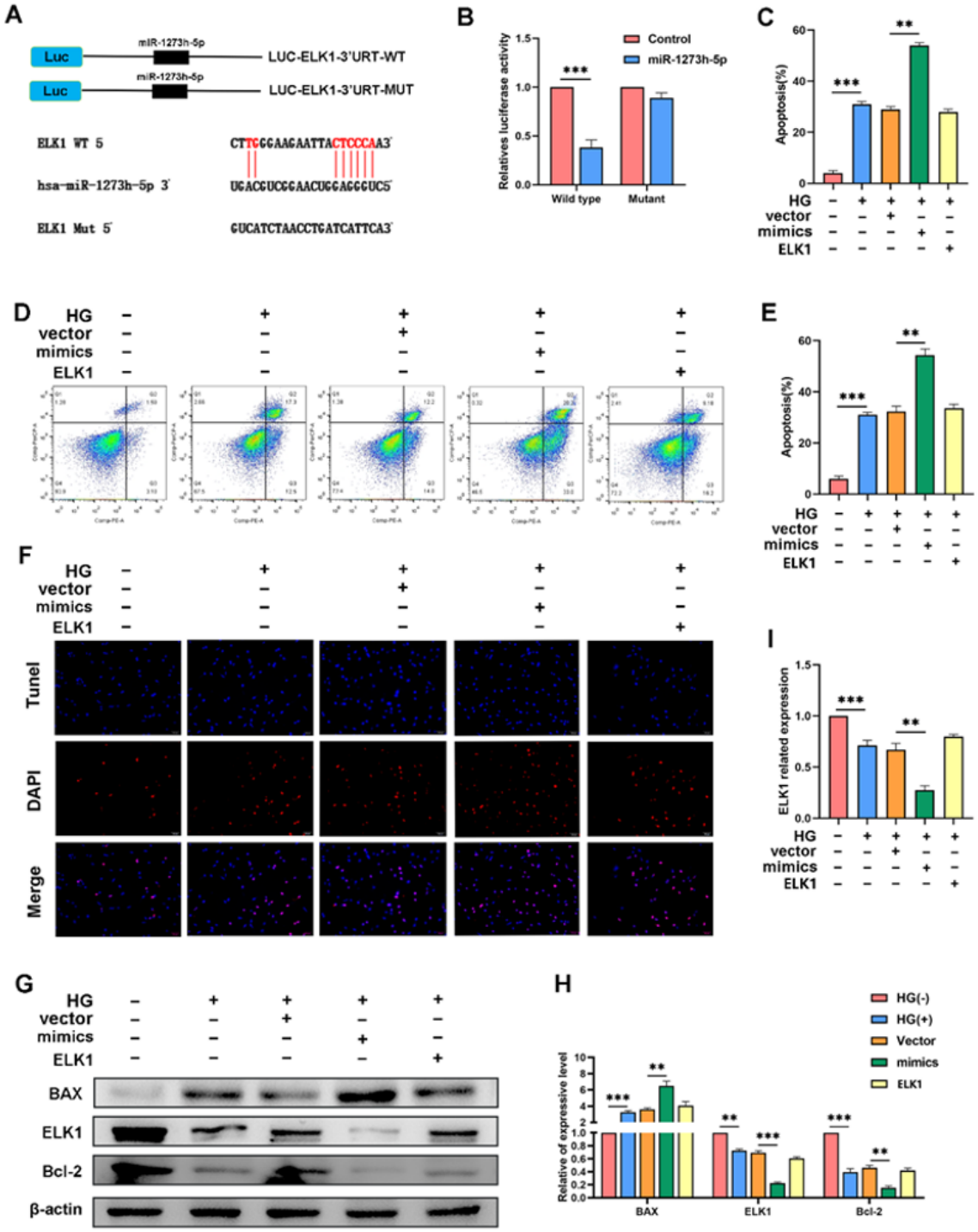

Figure 4

MiR-1273h-5p advanced ADSCs apoptosis through targeting ELK1. A, B. miR-1273h-5p bound ELK1 for dual luciferase assays were shown. C, D. After transfecting the miR-1273h-5p mimics and ELK1 plasmids

to ADSCs, the apoptosis of the cells was identified via flow cell technique. E, F. The programmed cell death was identified via TUNEL assay. G, H. Western blot experiment detected apoptosis-related proteins BAX, ELK1, BCL-2. I. The mRNA expressing of ELK1 was verified via qRT-PCR posterior to transferring miR-1273h-5p mimics into ADSCs. Scale bar = 50 μm. *p < 0.05, **p < 0.01, ***p < 0.001.

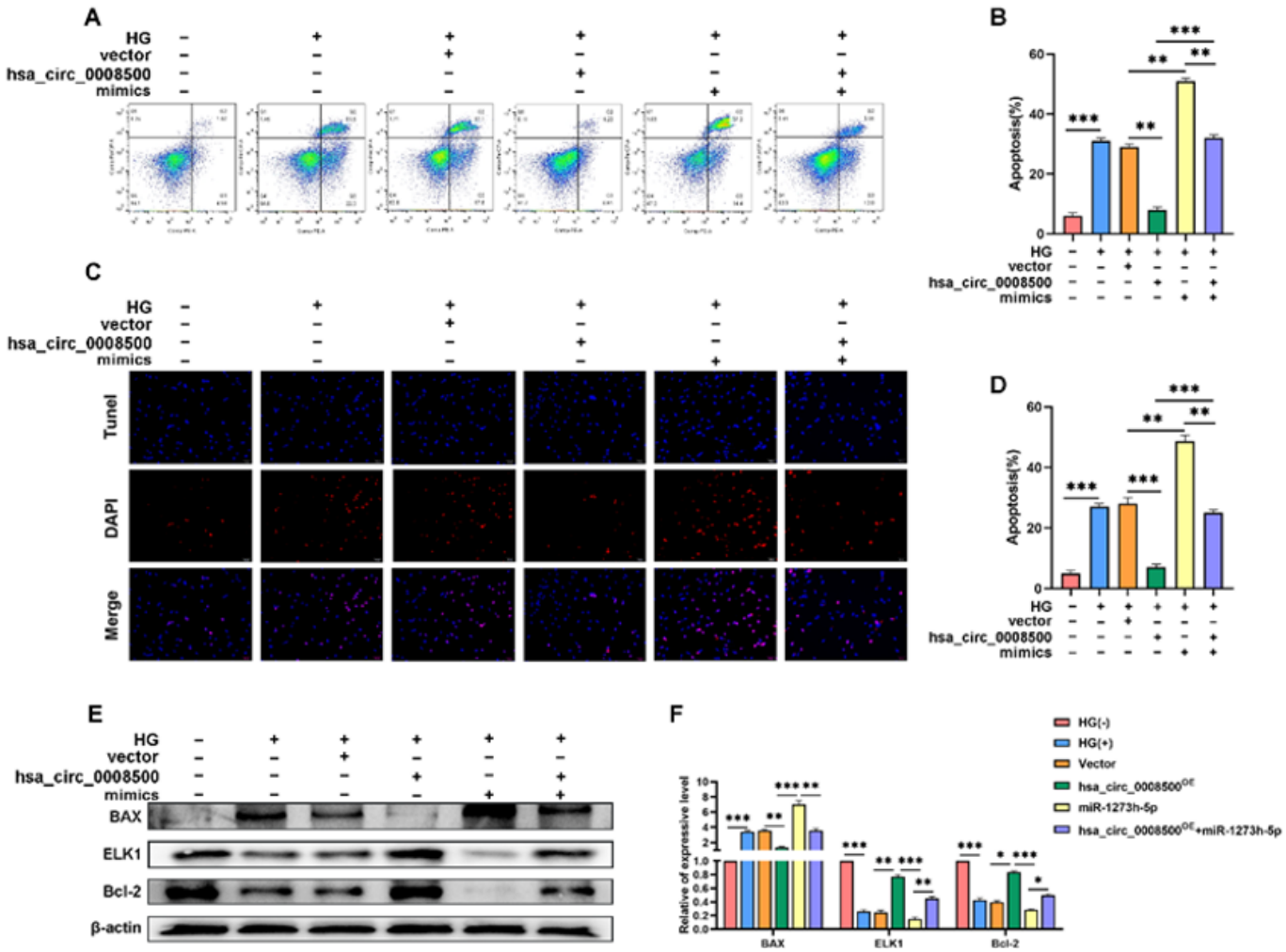

Figure 5

Hsa_circ_0008500 regulates ADSCs apoptosis via hsa-miR-1273h-5p. A. The hsa-miR-1273h-5p mimic plasmid was transferred into ADSCs and the apoptosis of ADSCs was identified via flow cell technique. B. Statistic analyses of flow cell technique. C. The TUNEL assay detected apoptosis. D. Statistical analysis of the TUNEL assay. E. Western blot experiment detected proteins BAX, ELK1, BCL-2. F. Statistical analysis of proteins BAX, ELK1, BCL-2. Scale bar = 50 μm. *p < 0.05, **p < 0.01, ***p < 0.001.